Available online at www.sciencedirect.com
SCIENCE DIRECT
Journal of Molecular Catalysis A: Chemical 241 (2005) 23–32
JOURNAL OF MOLECULAR CATALYSIS A: CHEMICAL
www.elsevier.com/locate/molcata

Catalysis of nanocrystalline mesoporous TiO_2 on cyclohexene epoxidation with H_2O_2: Effects of mesoporosity and metal oxide additives

Thammanoon Sreethawong [a], Yusuke Yamada [b,*], Tetsuhiko Kobayashi [b], Susumu Yoshikawa [a,**]

[a] *Institute of Advanced Energy, Kyoto University, Uji, Kyoto 611-0011, Japan*
[b] *Research Institute for Ubiquitous Energy Devices, National Institute of Advanced Industrial Science and Technology (AIST), 1-8-31 Midorigaoka, Ikeda, Osaka 563-8577, Japan*

Received 12 May 2005; received in revised form 1 July 2005; accepted 1 July 2005
Available online 5 August 2005

Abstract

Nanocrystalline mesoporous TiO_2-based catalysts prepared by a surfactant-assisted templating sol–gel process were tested on epoxidation of cyclohexene in *tert*-butanol–H_2O_2 system. The mesoporous TiO_2 showed exceptional potential for epoxidation of cyclohexene, exhibiting both higher cyclohexene conversion and higher cyclohexene oxide selectivity than non-mesoporous commercial TiO_2 powders, i.e. Ishihara ST-01 and Degussa P-25. The oxides of Fe, Co, Ni, and Ru were also loaded by incipient wetness impregnation method onto the synthesized mesoporous TiO_2, aiming to enhance the catalytic performance. Among metal oxide-loaded catalysts, RuO_2-loaded mesoporous TiO_2 was proved to possess noticeably high catalytic performance based on cyclohexene oxide selectivity. The 1 mol% RuO_2-loaded mesoporous TiO_2 was the best catalyst, showing the highest cyclohexene oxide selectivity and lowest cyclohex-2-en-1-ol (undesired product) selectivity. Plausible reaction pathways were also proposed.

Keywords: Mesoporosity; TiO_2; RuO_2; Epoxidation; Cyclohexene

1. Introduction

After mesoporous TiO_2 was first synthesized by a sol–gel process with phosphorous surfactants as templates by Antonelli and Ying [1], various methods of surfactant templating have been developed for the preparation of mesoporous structures of TiO_2 [2–4]. Since mesoporous materials normally possess large surface area and narrow pore size distribution, which advantageously make them a versatile candidate in the catalysis field, the utilization of mesoporous TiO_2 in many catalytic reactions becomes feasibly attractive. It is generally anticipated that the use of a high surface area mesoporous oxide support rather than a commercial support for noble or transition metals has some beneficial effects on the catalytic performance. The mesoporous support would give rise to well dispersed and stable metal particles on the surface upon calcination and reduction and as a consequence would show an improved catalytic performance [5].

Epoxidation reactions are indispensable for the chemical industry because of the ease, with which they can be used to convert olefins to oxygenated molecules, so-called epoxides, by oxygen transfer reaction. Epoxides are valuable and versatile commercial intermediates used as key raw materials for a wide variety of products owing to the numerous reactions they may undergo [6,7]. Epoxidation reactions of alkenes generally require the presence of a catalyst. However, several side reactions can take place, such as oxidation in the allylic positions, ring-opening of the epoxides by hydrolysis or solvolysis, epoxide rearrangement, or even total break-

* Corresponding author. Tel.: +81 72 751 9656; fax: +81 72 751 9630.
** Co-corresponding author. Tel.: +81 774 38 3504; fax: +81 774 38 3508.
E-mail addresses: Yusuke.YAMADA@aist.go.jp (Y. Yamada), s-yoshi@iae.kyoto-u.ac.jp (S. Yoshikawa).

1381-1169/$ – see front matter © 2005 Elsevier B.V. All rights reserved.
doi:10.1016/j.molcata.2005.07.009

down of the C=C double bonds. Cyclohexene epoxidation to yield cyclohexene oxide is one of the most difficult cases, in which the first two problems, namely allylic oxidation and epoxide ring-opening, occur considerably. As cyclohexene oxide is an important organic intermediate consumed in the production of pharmaceuticals, plant-protection agents, pesticides, and stabilizers for chlorinated hydrocarbons [8], much effort has been dedicated to the development of new active and selective cyclohexene epoxidation catalysts that circumvent the side reactions and the subsequent formation of large amounts of by-products.

Following the success in the synthesis of microporous titanosilicate catalysts, such as TS-1 for the selective oxidation of many organic compounds with H_2O_2 [9,10], titanium-containing catalysts, such as Ti-silicas and Ti-zeolites have been widely studied for the cyclohexene epoxidation [11–14], because titanium is capable of generating peroxometal intermediates, which facilitate the oxygen transfer to cyclohexene. Its oxide form, titanium oxide or titania (TiO_2), has been also greatly utilized as a support for vapor-phase epoxidation of propylene [15,16]. However, to our knowledge, the utilization of TiO_2, especially, with mesoporous structure in the cyclohexene epoxidation has not yet been intensely investigated. Since TiO_2 has been extensively used in multiple applications in the field of catalysis, especially, photocatalysis [17,18] and its surface contains a number of OH groups behaving as the sites for the formation of peroxotitanium complexes, it has been believed to be one of the active catalysts for the considered epoxidation reaction.

Recently in our previous work, the nanocrystalline mesoporous TiO_2 synthesized by a surfactant-assisted templating sol–gel system of tetraisopropyl orthotitanate modified with acetylacetone in the presence of laurylamine hydrochloride behaving as a mesopore-directing agent was reported [19]. In this work, the mesoporous TiO_2 synthesized by this combined sol–gel process with surfactant template was for the first time applied as an active catalyst for cyclohexene epoxidation in *tert*-butanol–H_2O_2 system. The synthesized mesoporous TiO_2 exhibited superior catalytic performance to non-mesoporous commercial TiO_2 powders, i.e. Ishihara ST-01 and Degussa P-25, in terms of both cyclohexene conversion and cyclohexene oxide selectivity. The effect of many metal oxide additives loaded onto the mesoporous TiO_2 was also investigated. RuO_2 was preliminarily found to be very efficient additive, and its optimum amount was sought. The plausible reaction pathways were also proposed based on the experimental observations.

2. Experimental

2.1. Catalyst synthesis

Typical synthesis procedure of mesoporous TiO_2 catalyst was explained in our previous report [19]. In brief, a specified amount of acetylacetone (abbreviated as ACAC) was first introduced into tetraisopropyl orthotitanate (abbreviated as TIPT) with the same mole. Afterwards, 0.1 M laurylamine hydrochloride (abbreviated as LAHC) aqueous solution was added into the ACAC-modified TIPT solution, in which the molar ratio of TIPT to LAHC was adjusted to a value of 4. The mixture was kept continuously stirring at 40 °C overnight to obtain transparent yellow sol. Then, the gel was formed by placing the TiO_2 sol into an oven kept at 80 °C for 1 week. Subsequently, the gel was dried overnight at 80 °C to eliminate the solvent. The dried sample was calcined at 500 °C for 4 h to remove LAHC template, and consequently, produce the mesoporous TiO_2. Metal oxide (Fe, Co, Ni, and Ru oxides)-loaded TiO_2 catalysts were prepared by incipient wetness impregnation of the synthesized mesoporous TiO_2 with an appropriate amount of the corresponding metal nitrate [$Fe(NO_3)_3{\cdot}9H_2O$, $Co(NO_3)_2{\cdot}6H_2O$, $Ni(NO_3)_2{\cdot}6H_2O$, and $Ru(NO)(NO_3)_3$] aqueous solution. The impregnated TiO_2 catalysts were then dried at 80 °C and finally calcined at 500 °C for 6 h.

2.2. Catalyst characterizations

X-ray diffraction (XRD) was used to identify phases present in the calcined samples. A Rigaku RINT-2100 rotating anode XRD system generating monochromated Cu Kα radiation with continuous scanning mode at rate of 2°/min and operating conditions of 40 kV and 40 mA was used to obtain XRD patterns. A nitrogen adsorption system (BEL Japan BELSORP-18 Plus) was employed to measure adsorption–desorption isotherms at liquid nitrogen temperature of −196 °C. The Brunauer–Emmett–Teller (BET) approach using adsorption data over the relative pressure ranging from 0.05 to 0.35 was utilized to determine specific surface area. The Barrett–Joyner–Halenda (BJH) approach was used to yield mean pore size and pore size distribution from desorption data. The sample was degassed at 200 °C for 2 h to remove physisorbed gases prior to the measurement. The sample morphology was observed by a transmission electron microscope (TEM, JEOL JEM-200CX) and a scanning electron microscope (SEM, JEOL JSM-6500FE) operated at 200 and 15 kV, respectively. The elemental mapping over the desired region of the catalyst was detected by an energy-dispersive X-ray spectrometer (EDS) attached to the SEM.

2.3. Catalytic activity measurement

The catalytic activity test was carried out without precautions against atmospheric air containing oxygen. Within a round-bottom glass reactor fitted with a reflux condenser and placed in a temperature-controlled chamber, the catalyst (20 mg) was added to a solution of cyclohexene (0.5 ml, 5 mmol) in *tert*-butanol (5 ml). The reaction mixture was magnetically stirred at 1000 rpm and heated under reflux until the reaction temperature (60 °C) was finally maintained. The reaction was then started by the addition of 30 wt.% aqueous H_2O_2 (0.1 ml, 1.25 mmol) into the mixture. After 3 h

of further stirring, aliquot was withdrawn from the reaction mixture, filtered, and subjected to a gas chromatograph (Shimadzu, GC-14B, Porapack Q, N_2 as carrier gas) equipped with a flame ionization detector (FID) for determination of product composition. Control experiments, reacting cyclohexene in *tert*-butanol with H_2O_2 in the absence of catalyst, were also comparatively performed. Identification of the products was examined using a gas chromatograph–mass spectrometer (Hewlett Packard, G1800A) with an electron ionization detector. The analysis revealed that the main products from the reaction are cyclohexene oxide (desired product), cyclohex-2-en-1-ol (undesired product), and cyclohex-2-en-1-one (undesired product). Selectivity is always given with respect to the converted cyclohexene. For the sake of comparison, the catalytic activity test with the commercially available non-mesoporous TiO_2 powders, i.e. Ishihara ST-01 and Degussa P-25, was also investigated.

3. Results and discussion

3.1. Catalyst characterizations

The N_2 adsorption–desorption measurement at liquid N_2 temperature of 77 K was used to study mesoporosity of the catalysts. Fig. 1 depicts the N_2 adsorption–desorption isotherm and pore size distribution of the synthesized TiO_2 catalyst, compared with the isotherms of Ishihara ST-01 and Degussa P-25. The isotherm of the synthesized TiO_2 in Fig. 1(a) revealed a typical type IV sorption behavior, representing the predominant mesoporous structure characteristic according to the classification of IUPAC [20]. A sharp increase in adsorption volume of N_2 was observed and located in the P/P_0 range of 0.45–0.85. This sharp increase can be attributed to the capillary condensation, indicating the good homogeneity of the sample and fairly small pore size since the P/P_0 position of the inflection point is related to the pore size. As shown in the inset of Fig. 1(a), the pore size distribution obtained from BJH method was very narrow and monomodal in the mesopore region (2–50 nm), indicating the good quality of the mesoporous catalyst prepared by this synthetic system. All loaded TiO_2 catalysts also exhibited this IUPAC type IV sorption pattern of mesoporous characteristic with narrow pore size distribution. In contrast, the isotherms of both commercial TiO_2 powders in Fig. 1(b) were completely different from that of the synthesized TiO_2 catalyst. Owing to IUPAC classification, they were associated with type II sorption behavior, which is generally obtained with non-porous or macroporous (large pore diameter of >50 nm) materials. Moreover, it has to be emphasized that this type of isotherm indicated the absence of predominant mesoporous structure in both commercial TiO_2 powders.

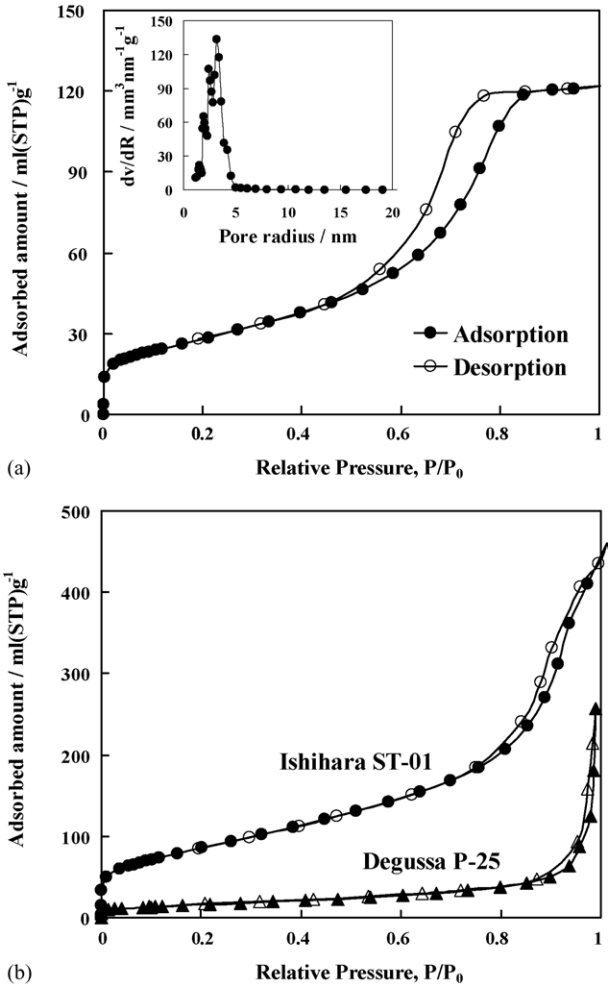

Fig. 1. (a) N_2 adsorption–desorption isotherm and mesopore size distribution (inset) of synthesized TiO_2 catalyst and (b) N_2 adsorption–desorption isotherms of Ishihara ST-01 and Degussa P-25.

The textural properties, namely BET surface area, mean pore diameter, and total pore volume, of the synthesized mesoporous TiO_2, Ishihara ST-01, and Degussa P-25 catalysts are comparatively given in Table 1. The mesoporous TiO_2 catalyst possessed quite high surface area of 101 $m^2\ g^{-1}$ with mean pore diameter and total pore volume of

Table 1
Textural properties and crystallite size of synthesized mesoporous TiO_2, Ishihara ST-01, and Degussa P-25 catalysts

Catalyst	BET surface area ($m^2\ g^{-1}$)	Mean pore diameter (nm)	Total pore volume ($cm^3\ g^{-1}$)	Crystallite size[b] (nm)
Mesoporous TiO_2	101	6.34	0.22	11.1
Ishihara ST-01	300	–[a]	–[a]	10.4
Degussa P-25	52	–[a]	–[a]	20.7 (Anatase), 29.9 (rutile)

[a] N_2 adsorption-isotherm corresponds to IUPAC type II pattern, indicating the absence of mesoporous structure.
[b] Estimated from line broadening of anatase (1 0 1) (and rutile (1 1 0) in case of Degussa P-25) diffraction peak using Sherrer formula.

Table 2
Textural properties and crystallite size of unloaded and 1 mol% metal oxide-loaded mesoporous TiO_2 catalysts

Catalyst	BET surface area ($m^2\ g^{-1}$)	Mean pore diameter (nm)	Total pore volume ($cm^3\ g^{-1}$)	Crystallite size (nm)
Unloaded TiO_2	101	6.34	0.22	11.1
FeO_x/TiO_2	82	8.38	0.21	11.6
CoO_x/TiO_2	74	8.38	0.21	12.7
NiO_x/TiO_2	76	8.38	0.21	12.5
RuO_2/TiO_2	73	8.38	0.20	13.5

6.34 nm (within mesopore region) and 0.22 $cm^3\ g^{-1}$, respectively. Even though there was no mesoporous characteristic observed in both commercial TiO_2 powders, the Ishihara ST-01 had about three-fold higher in surface area than the mesoporous TiO_2 but approximately half of the mesoporous TiO_2 in the case of Degussa P-25, which were resulted from specific commercial synthetic processes. When various 1 mol% metal oxide additives were loaded onto the mesoporous TiO_2, aiming to improve the catalytic performance, it can be seen that the BET surface area, mean pore diameter, and total pore volume as shown in Table 2 were insignificantly changed with varying the types of metal oxide additives, approximately 73–82 $m^2\ g^{-1}$, 8–9 nm, and 0.20–0.22 $cm^3\ g^{-1}$, respectively. Compared with the unloaded TiO_2, the TiO_2 catalysts with metal oxide additives exhibited less surface area and pore volume but larger pore size, primarily resulting from the stabilization of the mesoporous TiO_2 catalyst at 500 °C to remove surfactant template prior to the impregnation process, in which calcination step is required again at final stage to activate the metal oxide additives.

Since the catalytic activity test revealed that among loaded TiO_2 catalysts, RuO_2-loaded mesoporous TiO_2 provided the highest cyclohexene oxide (desired product) selectivity as shown later, the amount of RuO_2 loaded was varied up to 2 mol% to study the optimum loading amount. The textural properties of the RuO_2-loaded catalysts were also investigated as summarized in Table 3. It is obvious that the BET surface area gradually decreased with increasing the amount of RuO_2 loaded, plausibly due to the blockage of mesopore dimension with higher RuO_2 content. This subsequently caused the decrease in total pore volume, which was in the similar manner to the surface area. Nevertheless, the trend of mean pore diameter was relatively different. When 1 mol% RuO_2 was loaded onto the mesoporous TiO_2, the pore size was increased as previously explained that it could be attributable to the effect of two-step calcination. However, with further increase in the RuO_2 loading amount beyond 1 mol%, the pore size again became decreased to locate at slightly higher level than the unloaded mesoporous TiO_2. At these high loading amounts, the RuO_2 population may be sufficiently large to reduce the pore dimension, although the same two-step calcination was performed. In addition, it is worth noting that the pore diameter of all loaded catalysts was still in the mesopore region even after passing the loading and two-step calcination processes.

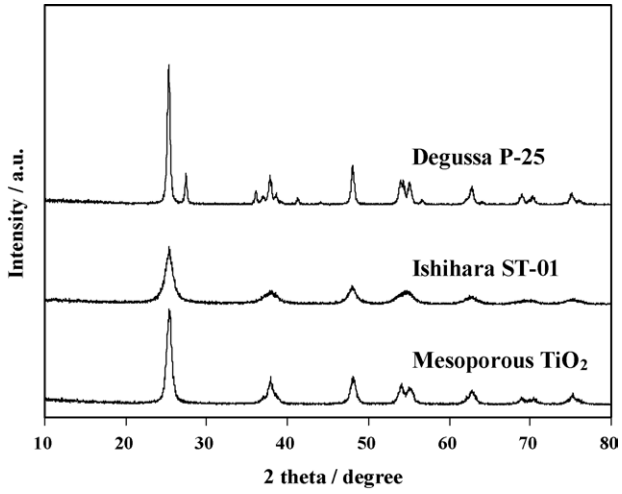

Fig. 2. XRD patterns of synthesized mesoporous TiO_2, Ishihara ST-01, and Degussa P-25 catalysts.

The crystalline phases of the catalysts were investigated using XRD analysis. The comparison of XRD patterns of the synthesized mesoporous TiO_2 with both commercial TiO_2 powders is shown in Fig. 2. The main peaks at 2θ of 25.2, 37.9, 47.8, 53.8, and 55.0°, which represent the indices of (1 0 1), (0 0 4), (2 0 0), (1 0 5), and (2 1 1) planes, respectively, are ascribed to structure of anatase TiO_2. It is evident that the mesoporous TiO_2 and Ishihara ST-01 structurally contained pure anatase phase. Besides, the diffractogram also shows that the mesoporous TiO_2 catalyst is highly crystalline. How-

Table 3
Textural properties and crystallite size of various mol% RuO_2-loaded mesoporous TiO_2 catalysts

Amount of RuO_2 loaded (mol%)	BET surface area ($m^2\ g^{-1}$)	Mean pore diameter (nm)	Total pore volume ($cm^3\ g^{-1}$)	Crystallite size (nm)
0	101	6.34	0.22	11.1
1	73	8.38	0.20	13.5
1.5	70	6.76	0.18	13.8
2	67	6.76	0.16	14.0

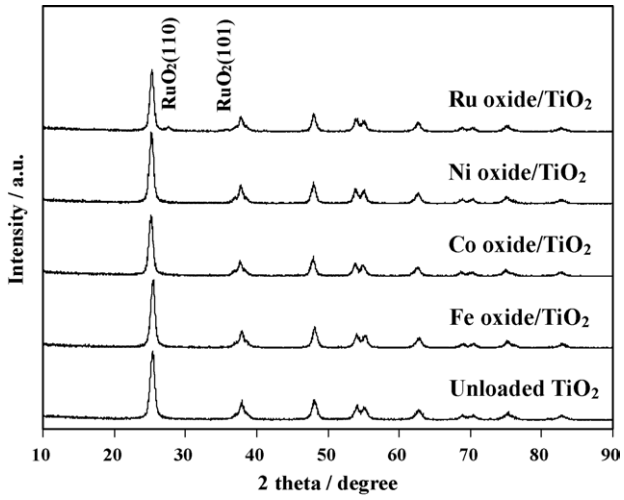

Fig. 3. XRD patterns of 1 mol% metal oxide-loaded mesoporous TiO_2 catalysts.

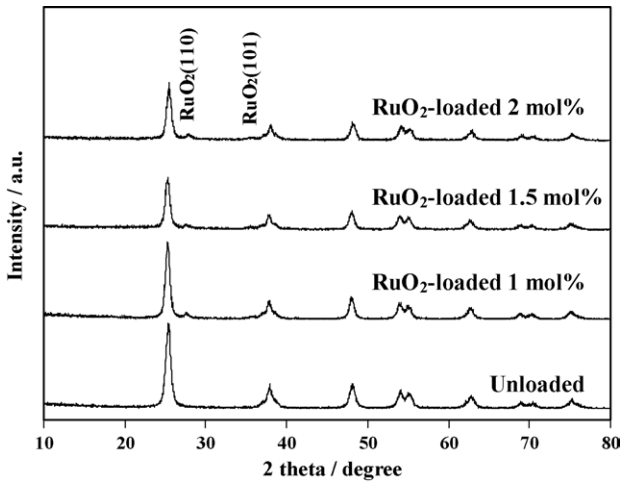

Fig. 4. XRD patterns of various mol% RuO_2-loaded mesoporous TiO_2 catalysts.

ever, in case of Degussa P-25, the existence of peaks at 2θ of 27.4, 36.1, 41.2, and 54.3°, which correspond to the indices of (1 1 0), (1 0 1), (1 1 1), and (2 1 1) planes, respectively, signifies the structure of rutile TiO_2. Hence, the Degussa P-25 structurally constitutes the mixture of anatase and rutile phases with 77% anatase content calculated using Spurr and Myers method [21]. The crystallite sizes of TiO_2 estimated from line broadening of anatase (1 0 1) diffraction peak (and also rutile (1 1 0) diffraction peak in case of Degussa P-25) using Sherrer formula [22] are presented in Table 1. The crystallite size of the mesoporous TiO_2 was about 11 nm, slightly larger than that of Ishihara ST-01. However, the average crystallite size of Degussa P-25 was approximately two-fold larger than that of the mesoporous TiO_2.

After being loaded with various 1 mol% metal oxides, the XRD patterns of the mesoporous TiO_2 catalysts are shown in Fig. 3. For the RuO_2-loaded mesoporous TiO_2, the presence of small diffraction peaks at 27.6° and 35.2° is indexed to RuO_2 (1 1 0) and (1 0 1) planes, respectively. However, the presence of diffraction peaks corresponding to other metal oxide additives, i.e. Fe, Co, and Ni oxides, could not be observed, probably due to the smaller content on a relative mass basis and high dispersion degree. Therefore, the mesoporous TiO_2 catalysts with these oxide additives are rather designated as FeO_x/TiO_2, CoO_x/TiO_2, and NiO_x/TiO_2, although the stable forms of these oxides under atmospheric air are Fe_3O_4, Co_3O_4, and NiO, respectively. The crystallite sizes of TiO_2 estimated from line broadening were approximately 11–14 nm as shown in Table 2. In the case of RuO_2-loaded mesoporous TiO_2 exhibiting the highest cyclohexene oxide selectivity as explained later, the XRD patterns of this catalyst with different amounts of RuO_2 loaded are depicted in Fig. 4. The loaded mesoporous TiO_2 still maintained highly crystalline anatase structure with the presence of RuO_2 phase detected. The crystallite size of the catalysts was relatively unchanged of about 14 nm as included in Table 3. From N_2 adsorption–desorption and XRD analyses, the synthesized TiO_2 catalyst by this synthetic method can be recognized as nanocrystalline mesoporous material.

The information about morphological structure of the synthesized catalyst could be obtained by both TEM and SEM analyses. As a representative, TEM image of 1 mol% RuO_2-loaded mesoporous TiO_2 catalyst shown in Fig. 5 demonstrated the formation of nanocrystalline TiO_2 aggregates composed of three-dimensional disordered primary particles. RuO_2 was observed as deposited particles dispersed on TiO_2 particles. The observed TiO_2 particle sizes of 10–15 nm were consistent with the crystallite size estimated from XRD analysis, elucidating that each grain corresponds in average to a single crystallite. In the same manner, the particle size of the RuO_2 single crystallite was approximately 2–3 nm with some aggregations. EDS focusing on the desired region of the catalyst under SEM operation was used to verify the disper-

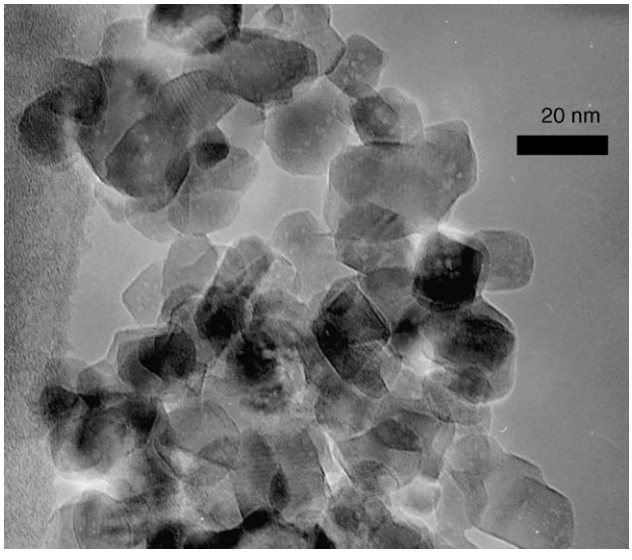

Fig. 5. TEM image of 1 mol% RuO_2/TiO_2 catalyst.

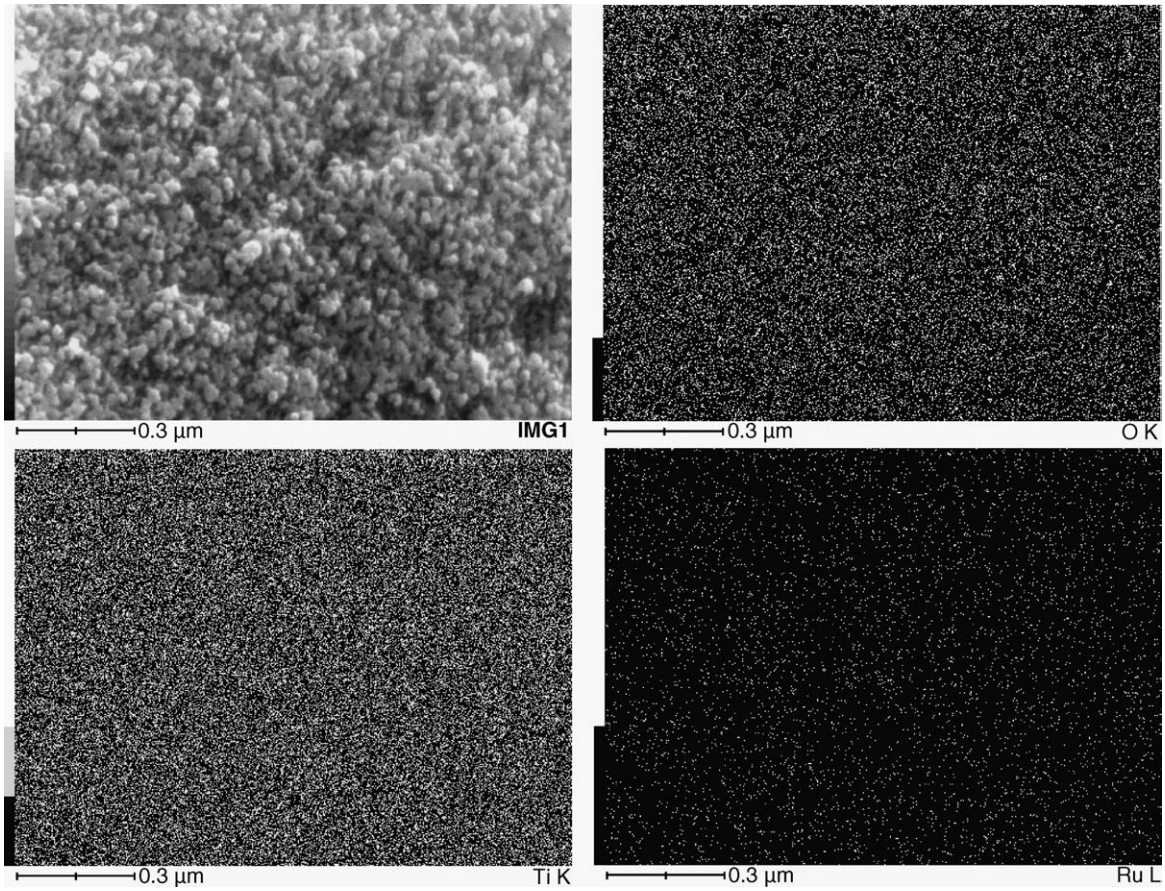

Fig. 6. SEM image and elemental mapping of 1 mol% RuO_2/TiO_2 catalyst.

sion of RuO_2 in the bulk materials. From elemental mapping mode as depicted in Fig. 6, highly and uniformly dispersed Ru-containing species through the bulk mesoporous TiO_2 were attained. In addition, the presence of highly mesoporous structure could also be evidently seen by SEM analysis. Owing to N_2 adsorption–desorption, TEM, and SEM results, the mesoporous structure of the synthesized catalyst can be attributed to the pores formed between nanocrystalline TiO_2 particles due to their aggregation, which is in the same line as the nanocrystalline mesoporous TiO_2 reported in several literatures [23–27].

3.2. Catalytic activity and reaction pathway

Epoxidation of cyclohexene was initially studied without (control) and with TiO_2 catalysts, i.e. synthesized mesoporous TiO_2, Ishihara ST-01, and Degussa P-25. The conversion and product selectivity results are shown in Fig. 7. After the reaction course, it was observed that in the absence of the catalyst, the auto-oxidation of cyclohexene occurred in the investigated system with cyclohexene conversion of 15% and comparable selectivity to cyclohexene oxide and cyclohex-2-en-1-ol. The cyclohexene conversion increased in the presence of the TiO_2 catalysts. It should be astonishingly noted that the mesoporous TiO_2 catalyst provided the highest cyclohexene conversion of 39%, approximately two-fold higher than that of both commercial TiO_2 powders. The cyclohexene oxide selectivity in the case of mesoporous TiO_2 was also higher. The product selectivity in the case of both commercial TiO_2 powders was rather varied with not only low cyclohexene oxide selectivity but also very high cyclohex-2-en-1-one selectivity. According to these preliminary results, the mesoporous TiO_2 catalyst was verified to have superior catalytic performance to both commercial TiO_2 powders in terms of both conversion and desired product selectivity. Although the Ishihara ST-01 possesses higher surface area than the mesoporous TiO_2, the mesoporosity contained in the synthesized TiO_2 seems to play much more significant role in enhancing reactant accessibility and surface reaction through the mesoporous structure. In case of the Degussa P-25, the absence of mesopore with low surface area as well as the presence of rutile phase can disadvantageously influence on the observed low catalytic performance. Even if the effect of rutile phase is not yet clearly understood, the less degree of hydroxylation (i.e. less number of surface hydroxyl groups) of the rutile structure rather than the anatase one [28–30] may be considered as a probable drawback in the formation of peroxotitanium complex. Therefore, it can be inferred that the synthesized nanocrystalline mesoporous TiO_2 is quite a promising catalyst for cyclohexene epoxidation.

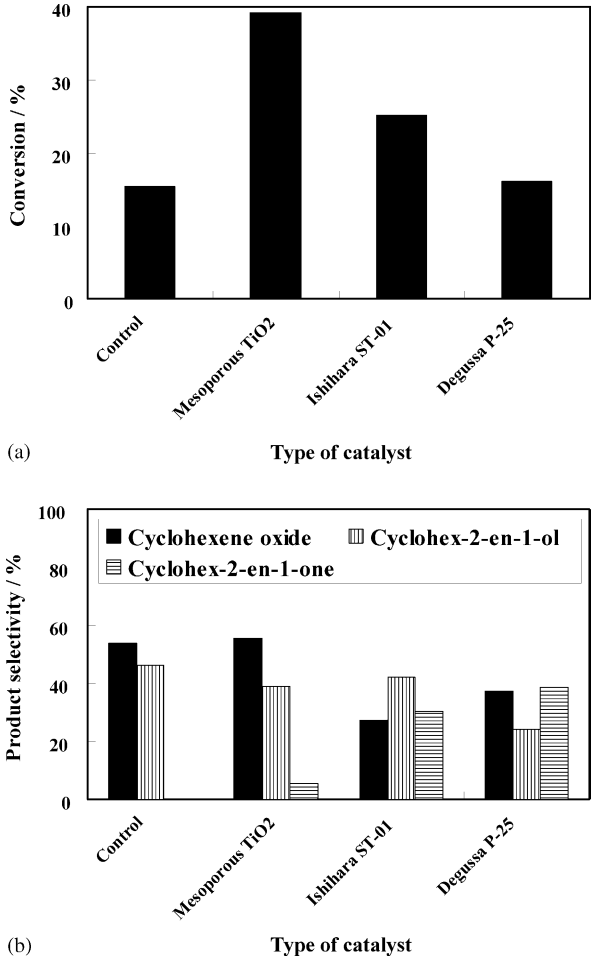

Fig. 7. Cyclohexene epoxidation catalyzed by synthesized mesoporous TiO_2, Ishihara ST-01, and Degussa P-25 catalysts: (a) cyclohexene conversion and (b) product selectivity.

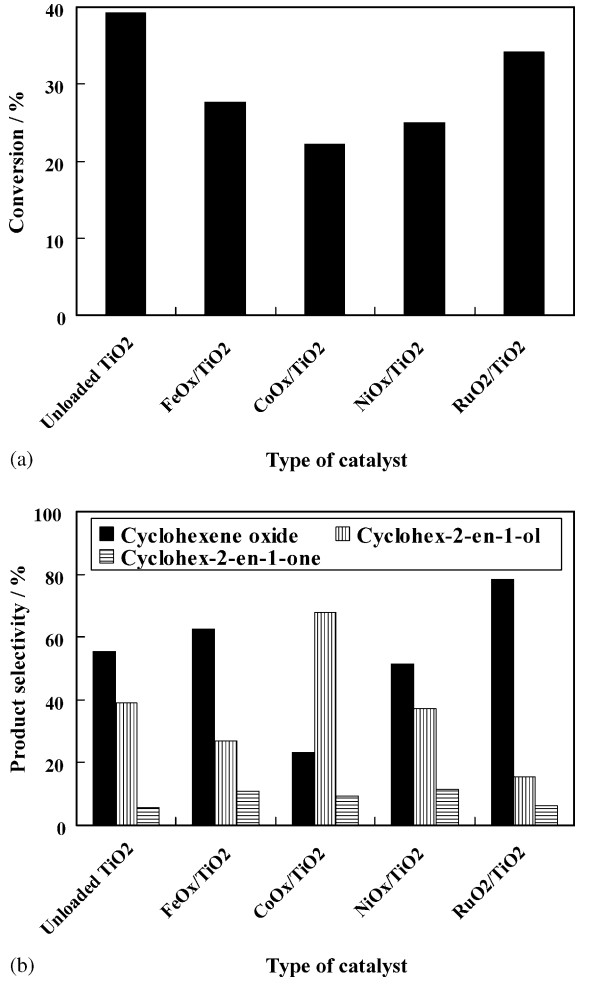

Fig. 8. Cyclohexene epoxidation catalyzed by 1 mol% metal oxide-loaded mesoporous TiO_2 catalysts: (a) cyclohexene conversion and (b) product selectivity.

Further study was focused on the effect of various 1 mol% metal oxide additives loaded onto the mesoporous TiO_2, intending to achieve the improvement of the catalytic performance. Fig. 8 shows the conversion and product selectivity results over these catalysts. It can be seen that although the loaded mesoporous TiO_2 provided somewhat lower cyclohexene conversion than the unloaded one, FeO_x- and RuO_2-loaded mesoporous catalysts showed higher cyclohexene oxide selectivity and lower cyclohex-2-en-1-ol selectivity. Particularly, RuO_2-loaded mesoporous TiO_2 gave the highest cyclohexene oxide selectivity up to 78.3% accompanying with relatively low cyclohex-2-en-1-ol selectivity of only 15.6%. In these comparative studies, CoO_x-loaded mesoporous TiO_2 catalyst showed the worst catalytic performance in this epoxidation reaction, yielding large amount of cyclohex-2-en-1-ol. Besides, NiO_x-loaded mesoporous TiO_2 catalyst exhibited only moderate catalytic performance compared with the RuO_2-loaded one, which allowed very high desired product selectivity with considerably low undesired product selectivity. As there were no dominant differences in their textural properties, it can be, therefore, pointed out that RuO_2-loaded mesoporous TiO_2 is an active catalyst in the investigated cyclohexene epoxidation reaction. From previous works, Ru-containing catalysts have also been found to be very effective for epoxidation reaction and used in many epoxidation systems [31,32].

Since high cyclohexene oxide selectivity is primarily focused as a target, the amount of RuO_2 loaded onto the mesoporous TiO_2 catalyst was considered as the main factor needed to be examined prior to further investigations. The RuO_2 loading amount was increased from 1 mol% as previously studied to 1.5 and 2 mol%, aiming to acquire the catalytic improvement. The conversion and product selectivity over these catalysts are illustrated in Fig. 9. Unfortunately, the increment in the amount of RuO_2 loaded beyond 1 mol% not only resulted in lower cyclohexene conversion but also lower cyclohexene oxide selectivity and higher undesired product selectivity. These results might be related to their textural properties shown in Table 3. As the pore size and pore volume were decreased in some extents when the RuO_2 loading amount was higher than 1 mol%, the reactant accessibility into the mesoporous structure could be reduced. The

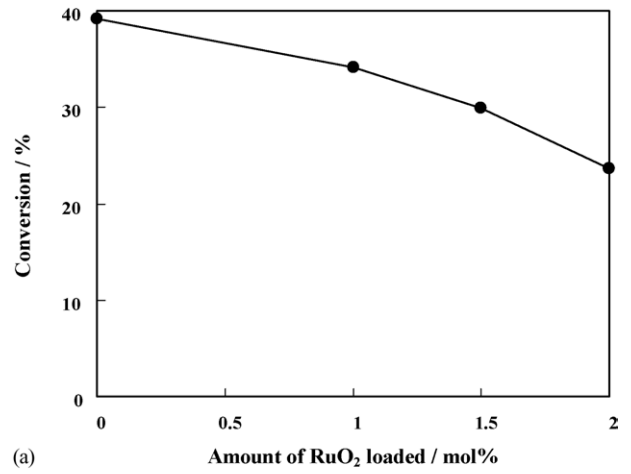

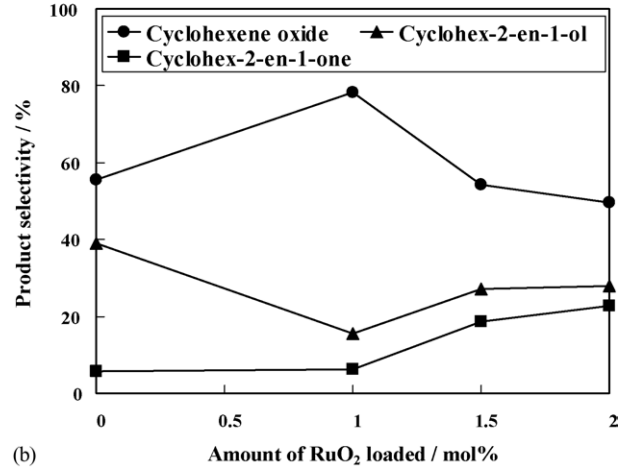

Fig. 9. Cyclohexene epoxidation catalyzed by various mol% RuO_2-loaded mesoporous TiO_2 catalysts: (a) cyclohexene conversion and (b) product selectivity.

less accessible reactants could lead to the lower cyclohexene conversion than that in the case of 1 mol% RuO_2-loaded catalyst. Because more extent of cyclohexene was left in the bulk solution outside the mesoporous reactive surface, it might undergo auto-oxidation more easily to yield higher undesired product contents, corresponding to higher undesired product selectivity. Hence, 1 mol% RuO_2-loaded mesoporous TiO_2 was evaluated as very active cyclohexene epoxidation catalyst in this investigated system, providing acceptably high cyclohexene oxide selectivity up to almost 80%.

Based on the experimental observations, the proposed pathway for cyclohexene epoxidation at TiO_2 surface is schematically shown in Fig. 10. As the reaction was performed in *tert*-butanol–H_2O_2 system with excess *tert*-butanol, *tert*-butyl hydroperoxide was expected to be abruptly in situ generated at the early stage. Upon the exposure of TiO_2 surface with this in situ generated *tert*-butyl hydroperoxide, *tert*-butyl peroxotitanium complex is formed because the apparent color change to yellowish was observed in case of all the bare TiO_2 powders, as also reported by Sensarma et al. on yellow peroxotitanium complex [33]. The peroxotitanium

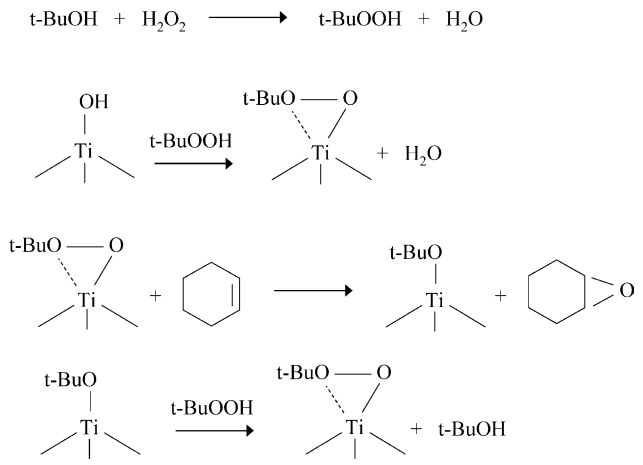

Fig. 10. Proposed pathway for cyclohexene epoxidation at TiO_2 surface.

complex (Ti–OH) formed by the direct reaction between TiO_2 and H_2O_2 should have been considered as another candidate for an active species, however, catalytic activity test in inert solvent of CH_3CN instead of *tert*-butanol showed only poor activity (14% conversion) and poor selectivity (6%) to cyclohexene oxide (20 mg catalyst, 0.5 ml cyclohexene, 0.1 ml H_2O_2, 60 °C, 3 h). This result suggested that the Ti-OO-*t*-Bu is a plausible active species. Additionally, although in case of the RuO_2-loaded mesoporous TiO_2 catalyst, the color change was not clearly observed as a result of the dull color of RuO_2, the formation of the *tert*-butyl peroxotitanium complex was supposed to also occur on the TiO_2 surface. The cyclohexene epoxidation is then proceeded by oxygen transfer from the *tert*-butyl peroxotitanium complex to the cyclohexene double bond. The consumed complex is finally regenerated by *tert*-butyl hydroperoxide. From the experimental results that among various catalysts the highest cyclohexene oxide selectivity was observed in the presence of the RuO_2-loaded mesoporous TiO_2 catalyst, the improvement of the selectivity due to the RuO_2 loading may be probably attributed to: (1) the assistance of RuO_2 to form the *tert*-butyl peroxotitanium complex and (2) the additional formation of *tert*-butyl peroxoruthenium complex due to the ability of ruthenium to form a variety of high-valent oxo complexes [31].

Furthermore, the observed result of cyclohexene conversion in the absence of catalyst shown in Fig. 7 implies that the auto-oxidation of cyclohexene was also taken place and accordingly accompanied with the epoxidation reaction in the presence of catalysts. The formation of cyclohexene oxide and cyclohex-2-en-1-ol during the reaction in the absence of catalyst suggests that free radical pathway is operative [34]. The proposed pathway for cyclohexene auto-oxidation is illustrated in Fig. 11. The liquid-phase auto-oxidation is ordinarily chain reaction of molecular O_2 and organic compound radicals initially produced by the reaction with an initiator. In this case, the in situ generated *tert*-butyl hydroperoxide functions as a major source of the initiator, which is thermally decomposed to generate active free radicals for auto-oxidation reaction. These free radicals then react

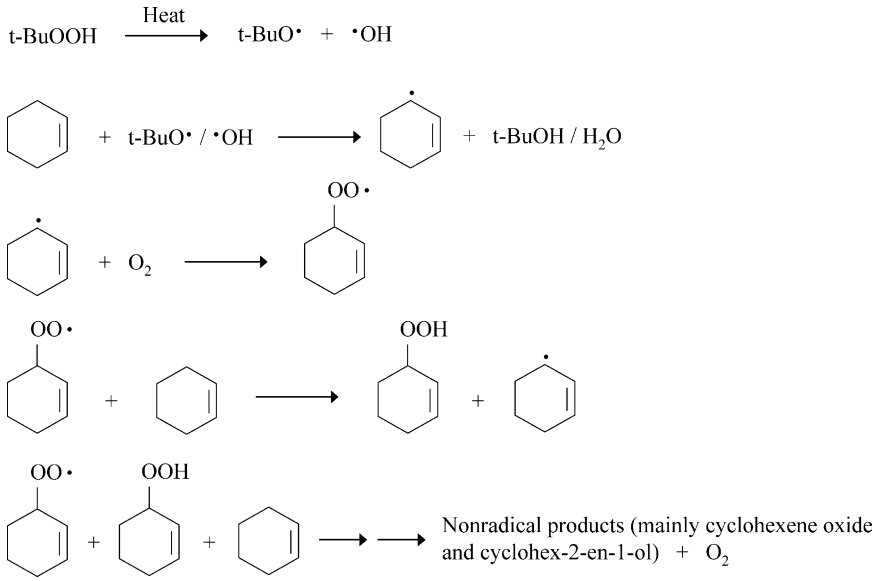

Fig. 11. Proposed pathway for cyclohexene auto-oxidation.

with cyclohexene to form organic compound radical, which is propagated through the reaction with molecular O_2 to form intermediate peroxide radical. Due to the low stability of this intermediate radical at the temperatures required for the reaction, it undertakes homolytic decomposition to afford non-radical products, mainly cyclohexene oxide and cyclohex-2-en-1-ol, since the primary products of olefin auto-oxidations are epoxides, alcohols, and carbonyl compounds [34]. Additionally, cyclohexene also inevitably undergoes the oxidation with the initiator radical, i.e. *tert*-butoxy radical, to form cyclohex-2-en-1-ol, which is further oxidized to cyclohex-2-en-1-one.

Overall, the mesoporous TiO_2 synthesized by this combined sol–gel process with surfactant template exhibited high potential to be used as cyclohexene epoxidation catalyst, compared with non-mesoporous Ishihara ST-01 and Degussa P-25. In this study, as to search the efficient metal oxide additive to improve its catalytic activity, high cyclohexene oxide selectivity could be attained over 1 mol% RuO_2-loaded mesoporous TiO_2. The ongoing works about the optimization of various experimental reaction conditions over this RuO_2-loaded catalyst are in progress in order to obtain better catalytic performance.

4. Conclusions

Nanocrystalline mesoporous TiO_2 catalyst with narrow monomodal pore size distribution was prepared via a surfactant-assisted templating sol–gel process of LAHC/TIPT modified with ACAC and utilized as cyclohexene epoxidation catalyst in *tert*-butanol–H_2O_2 system. The comparative activity tests showed that the synthesized mesoporous TiO_2 exhibited much better cyclohexene conversion and cyclohexene oxide selectivity than the non-mesoporous commercial TiO_2 powders, i.e. Ishihara ST-01 and Degussa P-25. The Fe, Co, Ni, and Ru oxide additives were loaded onto this mesoporous TiO_2 catalyst by incipient wetness impregnation process, aiming to increase its catalytic performance. It was found that 1 mol% RuO_2-loaded mesoporous TiO_2 catalyst was an active catalyst with satisfactory cyclohexene oxide selectivity. The reaction pathways, which could suitably explain the catalytic activity for the cyclohexene epoxidation, were also proposed.

Acknowledgements

This work was financially supported by the Grant-in-aid for Scientific Research from the Ministry of Education, Science, Sports, and Culture, Japan, under the 21 COE Program and the Nanotechnology Support Project. Grateful acknowledgments are forwarded to: (1) Prof. S. Isoda and Prof. H. Kurata and (2) Prof. T. Yoko at Institute for Chemical Research, Kyoto University, for their continuous support of the use of TEM and XRD apparatus, respectively.

References

[1] D.M. Antonelli, Y.J. Ying, Angew. Chem. Int. Ed. Engl. 34 (1995) 2014.
[2] D.M. Antonelli, Microporous Mesoporous Mater. 30 (1999) 315.
[3] P. Yang, D. Zhao, D.I. Margolese, B.F. Chmelka, G.D. Stucky, Chem. Mater. 11 (1999) 2813.
[4] H. Yoshitake, T. Sugihara, T. Tatsumi, Chem. Mater. 14 (2002) 1023.
[5] V. Idakiev, T. Tabakova, Z.Y. Yuan, B.L. Su, Appl. Catal. A Gen. 270 (2004) 135.
[6] C.W. Jones, Applications of Hydrogen Peroxide and Derivatives, RSC, Cambridge, 1999.
[7] R.A. Sheldon, M.C.A. van Vliet, in: R.A. Sheldon, H. van Bekkum (Eds.), Fine Chemicals through Heterogeneous Catalysis, Wiley, Weinheim, 2001.

[8] Technical Data Sheet, Chemical Divisions, BASF Corporation, 1997.
[9] M.G. Clerici, G. Bellussi, U. Romano, J. Catal. 129 (1991) 159.
[10] M.G. Clerici, P. Ingallina, J. Catal. 140 (1993) 71.
[11] T. Blasco, A. Corma, M.T. Navarro, J.P. Pariente, J. Catal. 156 (1995) 65.
[12] T. Maschmeyer, F. Rey, G. Sankar, J.M. Thomas, Nature 378 (1995) 159.
[13] A. Corma, P. Esteve, A. Martinez, S. Valencia, J. Catal. 152 (1995) 18.
[14] N. Jappar, Q. Xia, T. Tatsumi, J. Catal. 180 (1998) 132.
[15] T. Hayashi, K. Tanaka, M. Haruta, J. Catal. 178 (1998) 566.
[16] G. Mul, A. Zwijnenburg, B. van der Linden, M. Makkee, J.A. Moulijn, J. Catal. 201 (2001) 128.
[17] W.R. Moser, Advanced Catalysts and Nanostructured Materials, Academic Press, San Diego, 1996.
[18] A.L. Linsebigler, G. Lu, J.T. Yates Jr., Chem. Rev. 95 (1995) 735.
[19] T. Sreethawong, Y. Suzuki, S. Yoshikawa, J. Solid State Chem. 178 (2005) 329.
[20] F. Rouquerol, J. Rouquerol, K. Sing, Adsorption by Powders and Porous Solids: Principles, Methodology and Applications, Academic Press, San Diego, 1999.
[21] R.A. Spurr, H. Myers, Anal. Chem. 29 (1957) 760.
[22] B.D. Cullity, Elements of X-ray Diffraction, Addison-Wesley Publication Company, Reading, MA, 1978.
[23] J.C. Yu, J. Yu, W. Ho, L. Zhang, Chem. Commun. 19 (2001) 1942.
[24] J. Yu, J.C. Yu, M.K.P. Lueng, W. Ho, B. Cheng, X. Zhao, J. Zhao, J. Catal. 217 (2003) 69.
[25] Y. Zhang, A. Weidenkaff, A. Reller, Mater. Lett. 54 (2002) 375.
[26] Y. Zhang, H. Zhang, Y. Xu, Y. Wang, J. Solid State Chem. 177 (2004) 3490.
[27] Y.V. Kolen'ko, V.D. Maximov, A.V. Garshev, P.E. Meskin, N.N. Oleynikov, B.R. Churagulov, Chem. Phys. Lett. 388 (2004) 411.
[28] H.P. Maruska, A.K. Ghosh, Sol. Energy 20 (1978) 443.
[29] K. Tanaka, M.F.V. Capule, T. Hisanaga, Chem. Phys. Lett. 187 (1991) 73.
[30] R.I. Bickley, T. Gonzales-Carreno, J.L. Lees, L. Palmisano, R.J.D. Tilley, J. Solid State Chem. 92 (1991) 178.
[31] G.A. Barf, R.A. Sheldon, J. Mol. Catal. A Chem. 102 (1995) 23.
[32] S. Khare, S. Shrivastava, J. Mol. Catal. A Chem. 217 (2004) 51.
[33] S. Sensarma, A.O. Bouh, S.L. Scott, H. Alper, J. Mol. Catal. A Chem. 203 (2003) 145.
[34] R.A. Sheldon, J.K. Kochi, Metal-Catalysed Oxidation of Organic Compounds, Academic Press, NY, 1981.